Intrinsic Versus Extrinsic Anomalous Hall Effect in Ferromagnets

Shigeki Onoda,[1,*] Naoyuki Sugimoto,[2] and Naoto Nagaosa[2,3]

[1]*Spin Superstructure Project, ERATO, Japan Science and Technology Agency, c/o Department of Applied Physics, University of Tokyo, Tokyo 113-8656, Japan*

[2]*CREST, Department of Applied Physics, University of Tokyo, Tokyo 113-8656, Japan*

[3]*Correlated Electron Research Center, National Institute of Advanced Industrial Science and Technology, Tsukuba 305-8562, Japan*

(Received 23 May 2006; published 18 September 2006)

A unified theory of the anomalous Hall effect (AHE) is presented for multiband ferromagnetic metals with dilute impurities. In the clean limit, the AHE is mostly due to extrinsic skew scattering. When the Fermi level is located around anticrossing of band dispersions split by spin-orbit interaction, the intrinsic AHE to be calculated *ab initio* is resonantly enhanced by its nonperturbative nature, revealing the extrinsic-to-intrinsic crossover which occurs when the relaxation rate is comparable to the spin-orbit coupling.

DOI: 10.1103/PhysRevLett.97.126602 PACS numbers: 72.15.Eb, 72.15.Lh, 72.20.My, 75.47.−m

Early experimental works on the Hall effect in ferromagnetic metals led a semiempirical relation of the Hall resistivity ρ_{xy} to a *weak* applied magnetic field H and the spontaneous magnetization M both along the z direction; $\rho_{xy} = R_H H + 4\pi R_s M$ with the normal and the anomalous Hall coefficients R_H and R_s, respectively [1]. This anomalous Hall effect (AHE) [1] has been one of the most fundamental and intriguing but controversial issues in condensed-matter physics [2–7]. It has not been clarified yet if the AHE is originated purely from extrinsic scattering or has an intrinsic contribution from the electronic band structure, which penetrates even recent debates on the interpretation of the experiments [8–10]. Theoretically, a unified description of both intrinsic and extrinsic contributions is called for but has not been considered seriously. It even reveals their nontrivial interplay and crossover and explains the AHE in a whole region from the clean limit to the hopping-conduction region (see Fig. 4), which are the main goals of the present study.

The dissipationless and topological nature of the Hall effect has been highlighted by discovery of the quantum Hall effect [11] in two-dimensional electron systems under a *strong* magnetic field. In the Středa formula [12] of electric conductivity tensor $\sigma_{ij}^{\rm tot} = \sigma_{ij}^{I} + \sigma_{ij}^{II}$, in ideal case where the Fermi level is within the energy gap, the Fermi-surface part σ_{ij}^{I} vanishes and the quantum part σ_{ij}^{II} yields

$$\sigma_{ij}^{\rm TKNN} = -\epsilon_{ijl} e^2 \hbar \sum_n \int \frac{d^d \boldsymbol{p}}{(2\pi\hbar)^2} b_n^l(\boldsymbol{p}) f(\varepsilon_n(\boldsymbol{p})), \qquad (1)$$

with the electronic charge e, the Planck constant $h = 2\pi\hbar$, the Fermi distribution function $f(\varepsilon)$, and the antisymmetric tensor ϵ_{ijl} [13]. We have introduced the eigenenergy $\varepsilon_n(\boldsymbol{p})$, the Berry curvature $\boldsymbol{b}_n(\boldsymbol{p}) = \boldsymbol{\nabla}_p \times \boldsymbol{a}_n(\boldsymbol{p})$, and the Berry connection $\boldsymbol{a}_n(\boldsymbol{p}) = i\langle n, \boldsymbol{p}|\boldsymbol{\nabla}_p|n, \boldsymbol{p}\rangle$ of the generalized Bloch wave function $|n, \boldsymbol{p}\rangle$ with the band index n and the Bloch momentum $\boldsymbol{p}$. Each band has a topological integer called the Chern number $C_n \equiv -\int \frac{d^2\boldsymbol{p}}{(2\pi\hbar)^2} b_n^z(\boldsymbol{p})$. Their summation over the occupied bands determines the integer ν (Chern number) for the quantization $\sigma_{xy}^{\rm tot} = \nu e^2/h$ in insulators. Then, adiabatic semiclassical wave-packet equations have been devised to incorporate this Berry-curvature effect into the equations of motion [14].

Historically, Karplus-Luttinger [2] initiated an intrinsic mechanism of the AHE in a band model for ferromagnetic metals with the spin-orbit interaction, which coincides with $\sigma_{xy}^{\rm TKNN}$ [15]. This reflects that the spin-orbit interaction bears a nontrivial topological structure in the Bloch wave functions of ferromagnets by splitting band dispersions, which originally cross at a certain momentum $\boldsymbol{p}_0$, with a transfer of Chern numbers among the bands. This phenomenon called the ''parity anomaly'' has a nonperturbative nature [16], and points to an importance of the anticrossing points with a small gap $2\Delta_0$, which is identified with the spin-orbit interaction energy $\varepsilon_{\rm SO}$. When the Fermi level is located around such anticrossing of dispersions, as found in recent *ab initio* calculations for $SrRuO_3$ [17] and bcc Fe [18], the magnitude of $\sigma_{xy}^{\rm TKNN}$ is resonantly enhanced and approaches $e^2/h = 3.87 \times 10^{-5}\ \Omega^{-1}$ in two dimensions and $e^2/ha \sim 10^3\ \Omega^{-1}\,{\rm cm}^{-1}$ in three dimensions with lattice constant $a \approx 4$ Å [17,18].

On the other hand, adiabatic semiclassical Boltzmann transport analyses suggest that impurity scattering produces the AHE through the ''skewness'' [3,5,7] or the side jump [4,7]. The skew-scattering contribution diverges in the clean limit as $\sigma_{xy}^{\rm skew} = \sigma_{xx} S = \frac{2e^2}{ha} \frac{E_F \tau}{\hbar} S$ with the lifetime τ and the Fermi energy E_F. Here, $S \sim \varepsilon_{\rm SO} v_{\rm imp}/W^2 (\ll 1)$ is the skewness factor, with W being the bandwidth or the inverse of the density of states and $v_{\rm imp}$ the impurity potential strength.

A generic model that fully takes into account both the parity anomaly associated with the anticrossing of band dispersions and the impurity scattering can be obtained by

expanding the Hamiltonian at a fixed p_z with respect to the momentum $\boldsymbol{p}$ measured from the originally crossing point $\boldsymbol{p}_0$ of two dispersions;

$$\hat{H}_0 + \hat{H}_{\rm imp} = -\Delta_0 \hat{\sigma}^z + \lambda \boldsymbol{p} \cdot \hat{\boldsymbol{\sigma}} \times \boldsymbol{e}^z + \frac{\boldsymbol{p}^2}{2m} + v_{\rm imp} \sum_{\boldsymbol{r}_{\rm imp}} \delta(\boldsymbol{r} - \boldsymbol{r}_{\rm imp}), \quad (2)$$

with the position $\boldsymbol{r}$ of electron, the Pauli matrices $\hat{\boldsymbol{\sigma}} = (\hat{\sigma}_x, \hat{\sigma}_y, \hat{\sigma}_z)$, the unit vector $\boldsymbol{e}^z$ in the z direction, and an impurity at a position $\boldsymbol{r}_{\rm imp}$. The first term corresponds to the level splitting $2\Delta_0 = \varepsilon_{\rm SO}$ of two bands at the anticrossing momentum. The second term gives the linear dispersion with the velocity λ. The third term represents the quadratic dispersion with an effective mass m, whose anisotropy has been neglected since it is unimportant. This model has two band dispersions $\varepsilon_{\pm,\boldsymbol{p}}$ as shown in Fig. 1. Henceforth, the bottom of the lower band is chosen as the origin of the energy and the bottom of the upper band denoted as $E_{\rm res} = \varepsilon_-(0)$ is taken as an energy unit. The model possesses the gauge flux $b^z_{\pm,\boldsymbol{p}} = \mp\lambda^2\Delta_0/2\Delta^3_{\boldsymbol{p}}$ with $\Delta_{\boldsymbol{p}} = \sqrt{\lambda^2\boldsymbol{p}^2 + \Delta_0^2}$ [19,20]. In the case of resonance, $E_F \in [E_{\rm res} - 2\Delta_0, E_{\rm res}]$, $\sigma^{\rm TKNN}_{xy}$ approaches the maximum value $e^2/2h$. Away from this resonance, dominant contributions from the momentum region around $\boldsymbol{p} = 0$ cancel out each other or do not appear, leading to a suppression of $\sigma^{\rm TKNN}_{xy}(\approx (e^2/h) \times (\varepsilon_{\rm SO}/E_F))$, where the perturbation expansion in $\varepsilon_{\rm SO}$ is justified. Therefore, the present model, Eq. (2), can be regarded as a generic continuum model for a momentum region that gives a major contribution to the AHE. By definition of the anticrossing, Δ_0 does not change its sign as a function of p_z. This removes a concern that the integration over p_z might lead to a cancellation.

We employ the Keldysh formalism for nonequilibrium Green's functions, which has recently been reformulated for generic multicomponent systems [21]. We consider Green's functions and self-energies under an applied constant electric field $\boldsymbol{E} = (0, E_y)$; $\hat{G}^\alpha(\varepsilon, \boldsymbol{p})$ and $\hat{\Sigma}^\alpha(\varepsilon)$ with $\alpha = R, A, <$ for the retarded, advanced, and lesser components, respectively. ε and $\boldsymbol{p}$ represent the covariant energy and momentum in the Wigner representation [21]. $\hat{G}^\alpha(\varepsilon, \boldsymbol{p})$ and $\hat{\Sigma}^\alpha(\varepsilon)$ can be expanded in E_y as

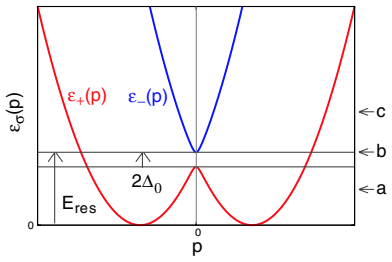

FIG. 1 (color online). Energy dispersions for $\hat{H}_0$ in Eq. (2).

$$\hat{G}^\alpha(\varepsilon, \boldsymbol{p}) = \hat{G}^\alpha_0(\varepsilon, \boldsymbol{p}) + e\hbar E_y \hat{G}^\alpha_{E_y}(\varepsilon, \boldsymbol{p}) + O(E_y^2), \quad (3)$$

$$\hat{\Sigma}^\alpha(\varepsilon) = \hat{\Sigma}^\alpha_0(\varepsilon) + e\hbar E_y \hat{\Sigma}^\alpha_{E_y}(\varepsilon) + O(E_y^2). \quad (4)$$

Henceforth, functionals with the subscripts 0 and E_y denote those in the absence of and the gauge-covariant linear response to E_y. Because of the δ-functional form of the impurity potential, the self-energies are local. $\hat{G}^{R,A}_0$ satisfies the familiar Dyson equation,

$$\hat{G}^{R,A}_0(\varepsilon, \boldsymbol{p}) = [\varepsilon - \hat{H}_0(\boldsymbol{p}) - \hat{\Sigma}^{R,A}_0(\varepsilon)]^{-1}. \quad (5)$$

The self-consistent equations for $\hat{G}^{R,A,<}_{E_y}$ are obtained by expanding the Dyson equation in the electric field [21]. It is convenient to decompose $\hat{G}^<_{E_y}$ and $\hat{\Sigma}^<_{E_y}$ into two;

$$\hat{G}^<_{E_y}(\varepsilon, \boldsymbol{p}) = \hat{G}^<_{E_y,I}(\varepsilon, \boldsymbol{p})\partial_\varepsilon f(\varepsilon) + \hat{G}^<_{E_y,II}(\varepsilon, \boldsymbol{p}) f(\varepsilon), \quad (6)$$

$$\hat{\Sigma}^<_{E_y}(\varepsilon) = \hat{\Sigma}^<_{E_y,I}(\varepsilon)\partial_\varepsilon f(\varepsilon) + \hat{\Sigma}^<_{E_y,II}(\varepsilon) f(\varepsilon), \quad (7)$$

$$\hat{G}^<_{E_y,II}(\varepsilon, \boldsymbol{p}) = \hat{G}^A_{E_y}(\varepsilon, \boldsymbol{p}) - \hat{G}^R_{E_y}(\varepsilon, \boldsymbol{p}), \quad (8)$$

$$\hat{\Sigma}^<_{E_y,II}(\varepsilon) = \hat{\Sigma}^A_{E_y}(\varepsilon) - \hat{\Sigma}^R_{E_y}(\varepsilon). \quad (9)$$

$\hat{G}^<_{E_y,I}$ and $\hat{\Sigma}^<_{E_y,I}$ can be self-consistently determined from the quantum Boltzmann equation in the first order in E_y,

$$[\hat{G}^<_{E_y,I}, \hat{H}_0] + \hat{G}^<_{E_y,I}\hat{\Sigma}^A_0 - \hat{\Sigma}^R_0\hat{G}^<_{E_y,I} = \hat{\Sigma}^<_{E_y,I}\hat{G}^A_0 - \hat{G}^R_0\hat{\Sigma}^<_{E_y,I} - \frac{i}{2}[\hat{v}_y, \hat{G}^A_0 - \hat{G}^R_0]_+ + \frac{i}{2}((\hat{\Sigma}^A_0 - \hat{\Sigma}^R_0)(\partial_{p_y}\hat{G}^A_0) + (\partial_{p_y}\hat{G}^R_0)(\hat{\Sigma}^A_0 - \hat{\Sigma}^R_0)), \quad (10)$$

with the velocity $\hat{v}_i(\boldsymbol{p}) = \partial_{p_i}\hat{H}_0(\boldsymbol{p})$, while $\hat{G}^{R,A}_{E_y}$ and $\hat{\Sigma}^{R,A}_{E_y}$ are determined from the other self-consistent equation,

$$\hat{G}^{R,A}_{E_y} = \hat{G}^{R,A}_0\hat{\Sigma}^{R,A}_{E_y}\hat{G}^{R,A}_0 - \frac{i}{2}(\hat{G}^{R,A}_0\hat{v}_y(\partial_\varepsilon\hat{G}^{R,A}_0) - (\partial_\varepsilon\hat{G}^{R,A}_0)\hat{v}_y\hat{G}^{R,A}_0). \quad (11)$$

We can exactly calculate the self-energies $\hat{\Sigma}^{R,A}_0$ and $\hat{\Sigma}^{R,A,<}_{E_y}$ up to the $n_{\rm imp}$-linear terms by means of the T-matrix approximation;

$$\hat{\Sigma}^{R,A}_0(\varepsilon) = n_{\rm imp}\hat{T}^{R,A}_0(\varepsilon), \quad (12)$$

$$\hat{T}^{R,A}_0(\varepsilon) = v_{\rm imp}\left(1 - v_{\rm imp}\int \frac{d^2\boldsymbol{p}}{(2\pi\hbar)^2}\hat{G}^{R,A}_0(\varepsilon, \boldsymbol{p})\right)^{-1}, \quad (13)$$

for the zeroth-order in E_y and

$$\hat{\Sigma}^<_{E_y,I}(\varepsilon) = n_{\rm imp}\hat{T}^R_0(\varepsilon)\int \frac{d^2\boldsymbol{p}}{(2\pi\hbar)^2}\hat{G}^<_{E_y,I}(\varepsilon, \boldsymbol{p})\hat{T}^A_0(\varepsilon), \quad (14)$$

$$\hat{\Sigma}^{R,A}_{E_y}(\varepsilon) = n_{\rm imp}\hat{T}^{R,A}_0(\varepsilon)\int \frac{d^2\boldsymbol{p}}{(2\pi\hbar)^2}\hat{G}^{R,A}_{E_y}(\varepsilon, \boldsymbol{p})\hat{T}^{R,A}_0(\varepsilon), \quad (15)$$

for the first order in E_y. We solve Eqs. (5), (12), and (13) self-consistently to obtain $\hat{G}_0^{R,A}$ and $\hat{\Sigma}_0^{R,A}$. Next, they are plugged into Eqs. (10) and (14) to solve $\hat{G}^<_{E_y,I}$ and $\hat{\Sigma}^<_{E_y,I}$ self-consistently. $\hat{G}^{R,A}_{E_y}$ and $\hat{\Sigma}^{R,A}_{E_y}$ are obtained from Eqs. (11) and (15), and hence $\hat{G}^<_{E_y,II}$ through Eq. (8). The conductivity tensors are calculated from

$$\sigma^I_{ij} = -\frac{e^2\hbar}{2\pi i}\int\frac{d^2\boldsymbol{p}}{(2\pi\hbar)^2}\,\mathrm{Tr}[\hat{v}_i(\boldsymbol{p})\hat{G}^<_{E_j,I}(E_F,\boldsymbol{p})], \tag{16}$$

$$\sigma^{II}_{ij} = e^2\hbar\int\frac{d\varepsilon}{2\pi i}\int\frac{d^2\boldsymbol{p}}{(2\pi\hbar)^2}\,\mathrm{Tr}[\hat{v}_i(\boldsymbol{p})\hat{G}^<_{E_j,II}(\varepsilon,\boldsymbol{p})]f(\varepsilon), \tag{17}$$

with $i, j = x, y$. Equations (16) and (17) are along the same spirit as the Středa formula [12]: this approach provides the diagrammatic treatment for the Středa formula [21]. Effects of the vertex corrections to $\hat{G}^<_{E_j,II}$ cancel each other, and hence we can regard σ^{II}_{xy} as an intrinsic contribution. The Fermi-surface contribution σ^I_{xy} suffers from a vertex correction. While the intraband matrix elements correspond to the conventional description of both σ_{xx} and σ_{xy} based on the scattering events, the interband ones contain an intrinsic contribution to the AHE as a part of the Berry-curvature term [22] and is generically expressed as

$$\sigma^{I\mathrm{int}}_{ij} = -\epsilon_{ijl}\frac{e^2\hbar}{2}\int\frac{d\boldsymbol{p}}{(2\pi\hbar)^d}\sum_{n,n'}(\varepsilon_n(\boldsymbol{p})-\varepsilon_{n'}(\boldsymbol{p}))\partial_\varepsilon f(\varepsilon_n(\boldsymbol{p})) \times \mathrm{Im}(\langle n\boldsymbol{p}|\boldsymbol{\nabla}_p|n'\boldsymbol{p}\rangle\times\langle n'\boldsymbol{p}|\boldsymbol{\nabla}_p|n\boldsymbol{p}\rangle)_l. \tag{18}$$

Figure 2(a) shows the numerical results on $\sigma^{\mathrm{tot}}_{xy} = \sigma^I_{xy} + \sigma^{II}_{xy}$ against the Fermi energy E_F and the Born scattering amplitude $\hbar/\tau \equiv n_{\mathrm{imp}}v^2_{\mathrm{imp}}m$ for a typical set of parameters, $\Delta_0 = 0.1$, $2mv_{\mathrm{imp}} = 0.6$, $2m\lambda^2 = 3.59$, and the energy cutoff is taken as $E_c = 3.0$ in an energy unit of $E_{\mathrm{res}} = 1.0$ [23]. In the clean limit $\hbar/\tau \to 0$, $\sigma^{\mathrm{tot}}_{xy}$ diverges in accordance with the skew-scattering scenario. The strength of the divergence is proportional to E_F in the low electron-density limit, and the sign is inverted around $E_F = \varepsilon_+(0) = E_{\mathrm{res}} - 2\Delta_0$. The sign of the skew-scattering contribution also changes by the sign change of v_{imp}. Figure 2(b) shows the intrinsic contribution $\sigma^{\mathrm{int}}_{xy}$ calculated by imposing $\hat{\Sigma}^{R,A,<}_{E_y} = 0$ for the same set of parameters. Under the resonant condition for E_F, $\sigma^{\mathrm{int}}_{xy}$ becomes of the order of $e^2/2h$. With increasing $\hbar/\tau$, it gradually decreases solely due to damping of quasiparticles.

By contrast, with increasing $\hbar/\tau$, the extrinsic skew-scattering contribution rapidly decays (Fig. 3), reflecting that it originates purely from intraband processes and hence the skewness factor S remains of the order of $\varepsilon_{\mathrm{SO}}v_{\mathrm{imp}}/W^2$. In moderately dirty cases, the total conductivity nearly merges into the intrinsic value: there appears a crossover from the extrinsic regime to the intrinsic as $\hbar/\tau$ increases. Especially in the resonant case shown in Fig. 3(b), the intrinsic contribution is significantly enhanced and the extrinsic-to-intrinsic crossover occurs at $\hbar/\tau \sim \varepsilon_{\mathrm{SO}}$. For a small ratio of $\varepsilon_{\mathrm{SO}}/E_F \sim 10^{-3}$–$10^{-2}$ [17,18], dominance of the intrinsic AHE is realized within the usual clean metal. In reality, the total Hall conductivity is the sum of the contributions from all over the Brillouin zone. Since skew-scattering contributions from other mo-

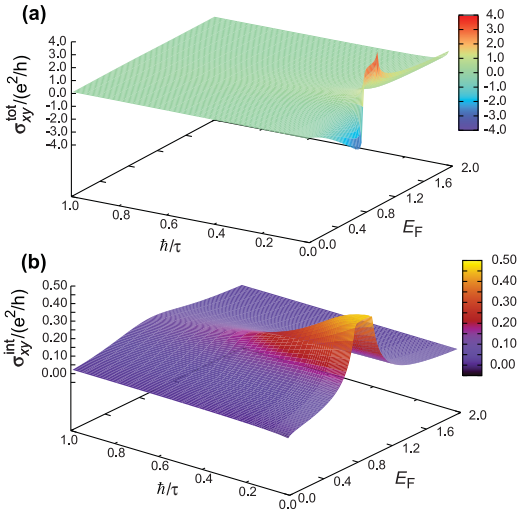

FIG. 2 (color). (a) The total anomalous Hall conductivity $\sigma^{\mathrm{tot}}_{xy}$ against E_F and $\hbar/\tau$ in an energy unit of $E_{\mathrm{res}} = 1.0$. (b) The intrinsic contribution $\sigma^{\mathrm{int}}_{xy}$ for the same parameter values. Note the difference of the scales for σ_{xy} in (a) and (b).

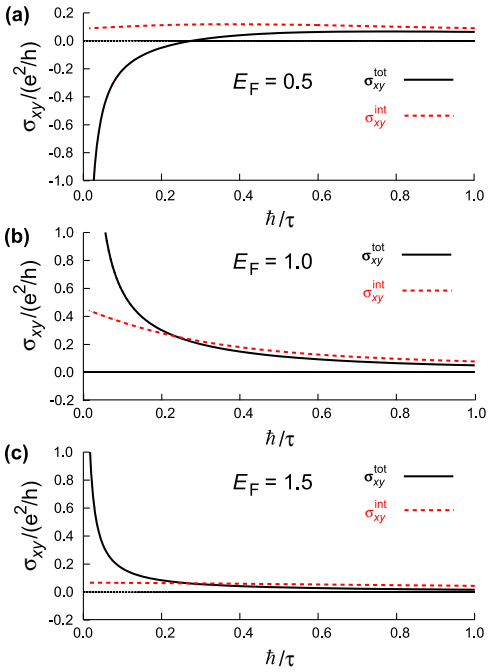

FIG. 3 (color online). $\sigma^{\mathrm{tot}}_{xy}$ and $\sigma^{\mathrm{int}}_{xy}$ as a function of $\hbar/\tau$ for the same parameter values as Fig. 2 with $E_F = 0.5$, 1.0, and 1.5 for (a), (b), and (c), respectively.

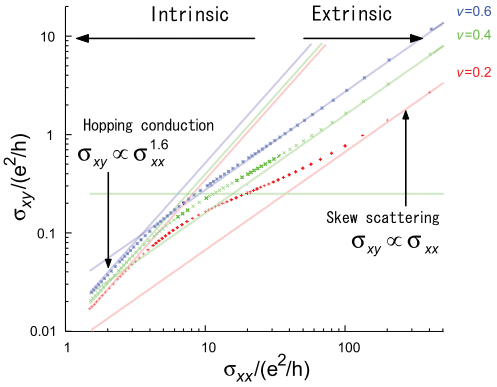

FIG. 4 (color). Scaling plot of σ_{xy} versus σ_{xx} for the same sets of parameter values as in Fig. 3(b) except $\nu = 2m v_{\rm imp}$.

mentum regions are always subject to a similar rapid decay, the above extrinsic-to-intrinsic crossover still occurs unless contributions from all the anticrossing regions of band dispersions are mutually canceled out by accident.

Figure 4 shows a logarithmic plot of σ_{xy} against σ_{xx} for the same set of parameters as Fig. 3(b) except for the impurity potential strength $v_{\rm imp}$, which is varied for different curves. In the clean limit, the curves nicely follow $\sigma_{xy} \propto \sigma_{xx}$ and the ratio σ_{xy}/σ_{xx} is proportional to $v_{\rm imp}$ for a fixed τ. As $\sigma_{xx} \sim 2(e^2/h)E_F\tau/\hbar$ decreases with decrease in τ, the relation exhibits an upward deviation from the linear one, signaling the crossover to the intrinsic regime. A smaller value of $v_{\rm imp}$ enlarges the region of the constant behavior of σ_{xy}. (Note that we change $n_{\rm imp}$ to control $\hbar/\tau$.) Careful experiments are required to test the prediction of the crossover at low temperatures. The magnitude of σ_{xy} in the intrinsic regime is consistent with experimentally observed values $\sigma_{xy} \cong 10^2 - 10^3\ \Omega^{-1}\,\mathrm{cm}^{-1}$ in a σ_{xy}-constant region of Fe- and Ni-based dilute alloys [1], and $SrRuO_3$ and metallic foils [24]. A further decrease of τ again changes the scaling behavior to $\sigma_{xy} \propto \sigma_{xx}^{1.6}$, which almost agrees with recent experiments on $Nd_2(Mo_{1-x}Nb_x)_2O_7$ [25] and on $La_{1-x}Sr_xCoO_3$ [24]. This exponent approximates to the value expected for the normal Hall effect in the hopping-conduction regime [26].

Now the source of the confusion over decades is clear. The skew-scattering contribution, though it is rather sensitive to details of the impurity potential and band structure, can be larger than e^2/h in the superclean case $\hbar/\tau \ll \varepsilon_{\rm SO}$, but decays for $\varepsilon_{\rm SO} < \hbar/\tau$. The side-jump contribution is smaller and of the order of $(e^2/h)(\varepsilon_{\rm SO}/E_F)$ [7]. Therefore, the intrinsic one, which is of the order of e^2/h under the resonant condition, is dominant over a wide range of the scattering strength $\varepsilon_{\rm SO} < \hbar/\tau < E_F$ (clean case). Although Luttinger reconsidered the Karplus-Luttinger theory [2] and gave an expansion of σ_{xy} in $v_{\rm imp}$, including the skew-scattering contribution as well [5], it fails to reveal the above crossover in the space of E_F, $\varepsilon_{\rm SO}$ and $\hbar/\tau$.

In conclusion, we have shown that the AHE is determined by the intrinsic mechanism when (i) the Fermi level is located around an anticrossing of band dispersions in the momentum space, (ii) consequently $\sigma_{xy} \sim e^2/(ha) \sim 10^3\ \Omega^{-1}\,\mathrm{cm}^{-1}$, and (iii) the resistivity ρ_{xx} is larger than $(ha/e^2)(\varepsilon_{\rm SO}/E_F) \sim 1$–$10\ \mu\Omega\,\mathrm{cm}$. With these conditions, first-principle calculation can give an accurate prediction of σ_{xy}. The present work resolves the long-standing controversy on the mechanism of the AHE in a whole region.

The authors thank A. Asamitsu, T. Miyazato, S. Iguchi, R. Mathieu, and Y. Tokura for discussion and showing unpublished experimental data, and H. Fukuyama, A. H. MacDonald, J. Sinova, J. Inoue, S. Murakami, K. Nomura, and M. Onoda for discussion. Numerics was performed using the supercomputer at the Institute of Solid State Physics, University of Tokyo. The work was supported by Grant-in-Aids (Grant No. 15104006, No. 16076205, and No. 17105002) and NAREGI Nanoscience Project from the Ministry of Education, Culture, Sports, Science, and Technology.

*Electronic address: sonoda@appi.t.u-tokyo.ac.jp

[1] C. M. Hurd, *The Hall Effect in Metals and Alloys* (Plenum, New York, 1972).
[2] R. Karplus and J. M. Luttinger, Phys. Rev. **95**, 1154 (1954).
[3] J. Smit, Physica (Amsterdam) **21**, 877 (1955).
[4] L. Berger, Phys. Rev. B **2**, 4559 (1970).
[5] J. M. Luttinger, Phys. Rev. **112**, 739 (1958).
[6] J. Kondo, Prog. Theor. Phys. **27**, 772 (1962).
[7] P. Nozieres and C. Lewiner, J. Phys. (Paris) **34**, 901 (1973).
[8] H. Ohno, Science **281**, 951 (1998).
[9] W.-L. Lee *et al.*, Science **303**, 1647 (2004).
[10] N. Manyala *et al.*, Nat. Mater. **3**, 255 (2004).
[11] *The Quantum Hall Effect*, edited by R. E. Prange and S. M. Girvin (Springer, Berlin, 1987).
[12] P. Středa, J. Phys. C **15**, L717 (1982).
[13] D. J. Thouless *et al.*, Phys. Rev. Lett. **49**, 405 (1982).
[14] G. Sundaram and Q. Niu, Phys. Rev. B **59**, 14 915 (1999).
[15] M. Onoda and N. Nagaosa, J. Phys. Soc. Jpn. **71**, 19 (2002); T. Jungwirth, Q. Niu, and A. H. MacDonald, Phys. Rev. Lett. **88**, 207208 (2002).
[16] R. Jackiw, Phys. Rev. D **29**, 2375 (1984).
[17] Z. Fang *et al.*, Science **302**, 92 (2003).
[18] Y. Yao *et al.*, Phys. Rev. Lett. **92**, 037204 (2004).
[19] V. K. Dugaev *et al.*, Phys. Rev. B **71**, 224423 (2005).
[20] N. A. Sinitsyn *et al.*, Phys. Rev. B **72**, 045346 (2005).
[21] S. Onoda, N. Sugimoto, and N. Nagaosa, Prog. Theor. Phys. **116**, 61 (2006), and references therein.
[22] N. A. Sinitsyn *et al.*, Phys. Rev. Lett. **97**, 106804 (2006)]
[23] Spin-dependent relaxation rate leads to $\sigma_{xy}^I \neq 0$ for $E_F > E_{\rm res}$ [J. Inoue *et al.*, Phys. Rev. Lett. **97**, 046604 (2006)].
[24] T. Miyazato *et al.* (private communication).
[25] S. Iguchi *et al.* (private communication).
[26] L. P. Pryadko and A. Auerbach, Phys. Rev. Lett. **82**, 1253 (1999).